



SPATIO-TEMPORAL SYNCHRONIZATION OF COUPLED PARAMETRICALLY EXCITED PENDULUM ARRAYS

Y. ZHANG AND G. H. DU

*Institute of Acoustics and State Key Laboratory of Modern Acoustics, Nanjing University,
Nanjing 210093, Republic of China. E-mail: zhudu@nju.edu.cn*

(Received 26 November 1999, and in final form 26 May 2000)

In this paper, parametrically excited chaotic pendulum arrays are considered with the spatial diffusive coupling. The drive array undergoes extremely irregular behavior, both temporally as well as spatially. To synchronize two coupled spatio-temporal chaotic arrays, the periodic feedback method is used. The synchronization condition is given to determine the critical values of periodic characteristic time and feedback weight. Furthermore, the influences of noise and parameter mismatch on synchronization are investigated. It is found that the periodic feedback method has strong robustness to noise and parameter mismatch, which promises its potential application in synchronizing parametrically excited pendulums.

© 2001 Academic Press

1. INTRODUCTION

The parametrically excited pendulum has received considerable attention recently [1–5]. Theoretical analysis and numerical simulations have revealed many complex time evolution phenomena such as bifurcation and chaos. Some of them have been shown in experimental investigations. However, for many realistic distributed systems, such as offshore platforms, buildings subject to earthquakes, etc., the problems involve both the temporal and spatial degrees of freedom. To give a more complete description, spatial characteristics should be considered. The coupled oscillator array can be described by a set of coupled differential equations with spatial convective coupling. As a kind of discrete-space model of the realistic distributed system, the coupled oscillator array provides insight into the nature of many non-linear phenomena. It has drawn the attention of theoretical and experimental researchers in physical, chemical, biological, neural network and other systems [6–9]. Therefore, the research on coupled parametrically excited pendulum array is very interesting and necessary.

In recent years, it has been found that despite the sensitivity to initial condition, two chaotic systems when certainly coupled can be synchronized, which has opened a new area of research [10–18]. Recently, spatio-temporal synchronization has received great interest [19–23]. Some continuous methods of chaotic synchronization such as the Pecora–Carroll method [10] have been generalized to synchronize spatio-temporal chaos of oscillator arrays, for which many interesting results have been obtained. However, in the practical applications of these methods, there are some important problems to be considered. First, noise and parameter mismatch will influence chaotic synchronization. This is clear since the inevitable inaccuracy of parameter and noise exist in any realistic environment, and can probably kick motion off the synchronization manifold. Furthermore, for the limitation in measurement, controlling chaotic response continuously often is unpracticed, and even

impossible. Control has to be activated in a kind of discontinuous way. Therefore, how to synchronize chaos under these conditions is significantly important for practical application.

In this paper, we investigate spatio-temporal chaotic synchronization of coupled parametrically excited pendulum arrays. Instead of the continuous feedback method [11], the periodic feedback scheme [5] is applied to synchronize two spatio-temporal chaotic arrays. The feedback is activated at discrete time, which can be described by the periodic characteristic time. By means of the spatial discrete Fourier transform, we obtain all the transverse Lyapunov exponents, so the synchronization condition can be given. Under this condition, the periodic feedback method synchronizes two spatio-temporal chaotic array systems well. Meanwhile, since noise and parameter mismatch of arrays exist in any experimental set-up of chaotic synchronization, the problem of how to perform a robust synchronization is very important to the practical realization. Through the investigation of noise and parameter mismatch, we find that the periodic feedback synchronization has strong robustness to these perturbations.

The contents of the paper are organized as follows: In sections 2 and 3, in order to make our research have more generality, we consider the general coupled oscillator arrays. The synchronization condition by the periodic feedback method is given in section 2. In section 3, we investigate the influence of noise and parameter mismatch. Finally, in section 4, based on the theoretical analysis, we perform the numerical calculation to synchronize parametrically excited pendulum arrays.

2. PERIODIC FEEDBACK SYNCHRONIZATION OF ARRAYS

To investigate the synchronization of coupled chaotic oscillator arrays, we consider a pair of unidirectionally coupled oscillator arrays with length N whose dynamics can be described as follows.

Drive array:

$$\dot{\mathbf{u}}_j = \mathbf{F}(\mathbf{u}_j, \mathbf{a}) + C\Gamma(\mathbf{u}_{j+1} + \mathbf{u}_{j-1} - 2\mathbf{u}_j), \quad j = 0, 1, \dots, N - 1, \tag{1}$$

Response array:

$$\dot{\tilde{\mathbf{u}}}_j = \mathbf{F}(\tilde{\mathbf{u}}_j, \tilde{\mathbf{a}}) + C\Gamma(\tilde{\mathbf{u}}_{j+1} + \tilde{\mathbf{u}}_{j-1} - 2\tilde{\mathbf{u}}_j) + K_f(t)\mathbf{I}(\mathbf{u}_j - \tilde{\mathbf{u}}_j) \tag{2}$$

and

$$K_f(t) = \begin{cases} 0, & n(\tau_1 + \tau_2) < t < n(\tau_1 + \tau_2) + \tau_1, \\ K, & n(\tau_1 + \tau_2) + \tau_1 \leq t < (n + 1)(\tau_1 + \tau_2), \end{cases} \quad n = 0, 1, \dots, \tag{3}$$

where $\mathbf{u}_j, \tilde{\mathbf{u}}_j \in \mathbf{R}^m$, and $\mathbf{F}: \mathbf{R}^m \rightarrow \mathbf{R}^m$ defines the non-linear vector field of a single oscillator. \mathbf{a} is the system parameter vector. N units of coupled chaotic oscillator build the oscillator arrays. Here, the nearest-neighbor diffusive coupling $C\Gamma(\tilde{\mathbf{u}}_{j+1} + \tilde{\mathbf{u}}_{j-1} - 2\tilde{\mathbf{u}}_j)$ is considered in the single oscillator array [21]. C is the coupling constant describing the diffusive action from the $j + 1$ unit and the $j - 1$ unit to the j unit. $\Gamma = \mathbf{1}, \mathbf{I} = \mathbf{1}$ are set to $n \times n$ unit diagonal matrixes. In order to synchronize the chaotic arrays (1) and (2), we apply the periodic feedback method $K_f(t)\mathbf{I}(\mathbf{u}_j - \tilde{\mathbf{u}}_j)$, where K is the feedback weight [5]. Feedback is added discretely: In the interval τ_1 , the arrays are independent; while in the interval τ_2 , the feedback is activated to synchronize two arrays. In sections 2 and 3, the periodic boundary condition $\mathbf{u}_j = \mathbf{u}_{j+N}$ is used. It is clear that equations (1) and (2) have the trivial solution $\dot{\mathbf{u}} = \mathbf{F}(\mathbf{u}, \mathbf{a})$. Then the stability of perturbation $\tilde{\mathbf{u}}_j - \mathbf{u}_j$ can be determined by the following

variational equation:

$$\dot{\xi}_j = \mathbf{DF}(\mathbf{u}, \mathbf{a})\xi_j + C\Gamma(\xi_{j+1} + \xi_{j-1} - 2\xi_j) - K_f(t)\mathbf{I}\xi_j, \tag{4}$$

where $\xi_j = \tilde{\mathbf{u}}_j - \mathbf{u}_j$ and $\mathbf{DF}(\mathbf{u})$ is the Jacobian of $\mathbf{F}(\cdot)$ evaluated at \mathbf{u} . Under the periodic boundary condition, equation (4) can be further diagonalized by performing the spatial Fourier transform $\xi_j = (1/\sqrt{N}) \sum_{k=0}^{N-1} \eta_k \exp(-2\pi ijk/N)$. Substituting the Fourier expansion into equation (4) and equating the coefficients for the eigenfunction, we have

$$\dot{\eta}_k = [\mathbf{DF}(\mathbf{u}, \mathbf{a}) - 4C\Gamma \sin^2(\pi k/N) - \mathbf{I}K_f(t)]\eta_k, \quad k = 0, 1, \dots, N - 1. \tag{5}$$

The solution of equation (5) can be integrated as [24, 21]

$$\eta_k(t) = T \exp\left[\int_0^t \mathbf{DF}(\mathbf{u}, \mathbf{a}) - \mathbf{I}K_f(\tau) d\tau\right] \exp[-4C\Gamma \sin^2(\pi k/N)t]\eta_k(0), \tag{6}$$

where T denotes the time evolution operator. It shows that two tendencies control the evolution of perturbation η_k . In the interval τ_1 , the response array is free from the drive array, so the perturbation can be written as

$$\begin{aligned} \eta_k [n(\tau_1 + \tau_2) + \tau_1] &= T \exp\left[\int_{n(\tau_1 + \tau_2)}^{m(\tau_1 + \tau_2) + \tau_1} \mathbf{DF}(\mathbf{u}, \mathbf{a}) d\tau\right] \exp[-4C\Gamma \sin^2(\pi k/N)\tau_1] \\ &\times \eta_k [n(\tau_1 + \tau_2)]. \end{aligned} \tag{7}$$

However, in the interval τ_2 , the feedback is active and the response array is driven by the feedback, so the perturbation satisfies

$$\begin{aligned} \eta_k [(n + 1)(\tau_1 + \tau_2)] &= T \exp\left[\int_{n(\tau_1 + \tau_2) + \tau_1}^{(n + 1)(\tau_1 + \tau_2)} \mathbf{DF}(\mathbf{u}, \mathbf{a}) d\tau\right] \exp[-(KI + 4C\Gamma \sin^2(\pi k/N))\tau_2] \\ &\times \eta_k [n(\tau_1 + \tau_2) + \tau_1] \end{aligned} \tag{8}$$

Combining these two equations, we obtain

$$\begin{aligned} \eta_k [(n + 1)(\tau_1 + \tau_2)] &= T \exp\left[\int_0^{(n + 1)(\tau_1 + \tau_2)} \mathbf{DF}(\mathbf{u}, \mathbf{a}) d\tau\right] \exp[-(n + 1)(\tau_1 + \tau_2)(4C\Gamma \sin^2(\pi k/N) + KI/D)] \eta_k(0), \end{aligned} \tag{9}$$

where $D = (\tau_1 + \tau_2)/\tau_2$ is defined as the periodic characteristic time. Clearly, $D = 1$ ($\tau_1 = 0$ or $\tau_2 \gg \tau_1$) presents the continuous situation. For coupled systems, the spectra of Lyapunov exponent can be divided into two subsets $\{\lambda_{k, sy}^i\}, \{\lambda_{k, tr}^i\}$ ($i = 1, 2, \dots, m, k = 0, 1, \dots, N - 1$), which correspond to the synchronization manifold and the transverse to this manifold. The first one $\{\lambda_{k, sy}^i\}$ describes the drive array, while the second one $\{\lambda_{k, tr}^i\}$ is known as the transverse Lyapunov exponents that describe the perturbations along transverse directions of the synchronization manifold. The positive transverse Lyapunov exponents tend to kick the trajectory off synchronization manifold so that the trajectory will wander in a high-dimensional phase space. Therefore, the synchronization problem is to let all the transverse Lyapunov exponents $\lambda_{k, tr}^i < 0$. Since the eigenvalues μ_0^i ($i = 1, 2, \dots, m$) of $\lim_{n \rightarrow \infty} [T \exp(\int_0^{(n + 1)(\tau_1 + \tau_2)} \mathbf{DF}(\mathbf{u}, \mathbf{a}) d\tau)]^{1/(n + 1)(\tau_1 + \tau_2)}$ are related to the Lyapunov exponents λ_0^i of the single oscillator $\dot{\mathbf{u}} = \mathbf{F}(\mathbf{u})$, $\lambda_{k, sy}^i$ can be given by $\lambda_{k, sy}^i = \lambda_0^i - 4C \sin(\pi k/N)$ [21]. It has been found that if the coupling constant C satisfies $\lambda_0^{max} - 4C \sin^2(\pi/N) < 0$, then all

the units of the single array have the trivial solution $\mathbf{u}_{j-1} = \mathbf{u}_j = \mathbf{u}_{j+1} = \mathbf{u}$ ($j = 0, 1, \dots, N - 1$). This phenomenon is called as spatial coherence [20, 21]. Under this condition, the array shows the homogeneity in space so that the dynamics of the array behaves as if there were an isolated chaotic oscillator. In this paper, in order to produce the complicated irregularity in space and time, we consider the weak coupling, i.e. $\lambda_0^{max} - 4C \sin^2(\pi/N) > 0$, then local perturbation will be amplified to the whole array. From equation (9), we have the transverse Lyapunov exponents to

$$\lambda_{k,tr}^i = \lambda_{k,sy}^i - K/D. \tag{10}$$

For $t \rightarrow \infty$, the evolution of $\langle \|\eta_k\| \rangle_u$ tends to fall along the most rapid growth corresponding to the maximal transverse Lyapunov exponent $\lambda_{k,tr}^{max} = \lambda_0^{max} - 4C \sin^2(\pi k/N) - K/D$, and then the average perturbation can be given

$$\langle \|\eta_k[(n + 1)(\tau_1 + \tau_2)]\| \rangle_u \sim \exp[(n + 1)(\tau_1 + \tau_2)(\lambda_0^{max} - 4C \sin^2(\pi k/N) - K/D)] \langle \|\eta_k(0)\| \rangle_u \tag{11}$$

where $\|\cdot\|$ denotes the Euclidean matrix norm, and $\langle \cdot \rangle_u$ is the ensemble averaged with respect to the initial condition $\mathbf{u}(0)$. Therefore, to synchronize arrays (1) and (2), we should have $\lambda_{k,tr}^{max} < 0$, that is,

$$D[\lambda_0^{max} - 4C \sin^2(\pi k/N)] < K. \tag{12}$$

Here, different eigensolutions η_k have their respective convergence conditions. Only when the feedback weight K is large enough, all eigensolutions η_k , including $k = 0$ solution η_0 , will decrease to zero. We then are sure to have the synchronization condition

$$D\lambda_0^{max} < K. \tag{13}$$

When the periodic characteristic time $D = 1$, the result can be reduced to that of the continuous feedback scheme of Pyragas [11]. If there exists a subset $B \subset R^{mN}$, so that for all initial conditions $\mathbf{u}(0), \tilde{\mathbf{u}}(0) \in B$, two arrays are synchronous $\eta_k \rightarrow 0, \xi_j \rightarrow 0$ with $n \rightarrow \infty$. Then we call this subset B as the synchronization manifolds.

It must be pointed out that the successful synchronization should guarantee the following conditions: (i) synchronization condition, equation (13), holds; and (ii) the trajectory remains within synchronization manifold B . Otherwise, if τ_1 is too large or τ_2 is too small, the trajectory may wander out of the synchronization manifolds so that we cannot synchronize two coupled arrays. From the synchronization condition, equation (13), we have the relationship of the critical values K_{min}, D_{max} :

$$K_{min} = D_{max} \lambda_0^{max}. \tag{14}$$

3. INFLUENCE OF NOISE AND PARAMETER MISMATCH

In coupled flow systems, perturbations including noise and parameter mismatch are extremely important for the evolution of spatio-temporal dynamics. Local perturbations will be amplified over the whole spatial extent through the diffusive coupling for the convective instability. In the experiment of synchronizing parametrically excited pendulums, noise and parameter mismatch exist inevitably in the practical environment. Therefore, the influence of these perturbations on synchronization should be investigated. Adding noise and parameter mismatch terms, we rewrite the perturbed variational

equations as

$$\begin{aligned} \dot{\xi}_j &= \mathbf{DF}(\mathbf{u}, \mathbf{a}) \xi_j + C\Gamma(\xi_{j+1} + \xi_{j-1} - 2\xi_j) - K_f(t)\mathbf{I}\xi_j + \mathbf{I}\zeta(t), \\ \dot{\xi}_j &= \mathbf{DF}(\mathbf{u}, \mathbf{a}) \xi_j + C\Gamma(\xi_{j+1} + \xi_{j-1} - 2\xi_j) - K_f(t)\mathbf{I}\xi_j + \mathbf{D}_a\mathbf{F}(\mathbf{u}_j, \mathbf{a})\Delta\mathbf{a}, \end{aligned} \tag{15}$$

where $\mathbf{D}_a\mathbf{F}(\mathbf{u}, \mathbf{a})$ is the Jacobian of $\mathbf{F}(\cdot)$ with respect to the parameter \mathbf{a} . $\Delta\mathbf{a} = \tilde{\mathbf{a}} - \mathbf{a}$ denotes parameter mismatch. Noise $\zeta(t)$ has mean value 0 and mean-squared value σ^2 . Carrying out the spatial Fourier transform to diagonalize the variational equation, we solve equation (15) as

$$\begin{aligned} \eta_k [(n + 1)(\tau_1 + \tau_2)] &= \eta_k [n(\tau_1 + \tau_2)] e^{[\tilde{\lambda}(\tau_1 + \tau_2) - K\Gamma\tau_2]} + e^{(\tilde{\lambda} - K\Gamma)\tau_2} \int_0^{\tau_1} e^{\tilde{\lambda}(\tau_1 - \tau)} \\ &\times \frac{1}{\sqrt{N}} e^{(2\pi ijk/N)} \mathbf{D}_a\mathbf{F}\Delta\mathbf{a} \, d\tau + \int_0^{\tau_2} e^{(\tilde{\lambda} - K\Gamma)(\tau_2 - \tau)} \frac{1}{\sqrt{N}} e^{(2\pi ijk/N)} \mathbf{D}_a\mathbf{F}\Delta\mathbf{a} \, d\tau \end{aligned} \tag{16}$$

and

$$\begin{aligned} \eta_k [(n + 1)(\tau_1 + \tau_2)] &= \eta_k [n(\tau_1 + \tau_2)] e^{[\tilde{\lambda}(\tau_1 + \tau_2) - K\Gamma\tau_2]} + e^{(\tilde{\lambda} - K\Gamma)\tau_2} \int_0^{\tau_1} e^{\tilde{\lambda}(\tau_1 - \tau)} \\ &\times \frac{1}{\sqrt{N}} e^{(2\pi ijk/N)} \zeta(\tau) \, d\tau + \int_0^{\tau_2} e^{(\tilde{\lambda} - K\Gamma)(\tau_2 - \tau)} \frac{1}{\sqrt{N}} e^{(2\pi ijk/N)} \zeta(\tau) \, d\tau, \end{aligned} \tag{17}$$

where $\tilde{\lambda} = \lambda - 4C\mathbf{I}\sin^2(\pi k/N)$ and λ is the diagonal matrix constructed from the eigenvalues μ_0^i , $i = 1, 2, \dots, m$. When $n \rightarrow \infty$, if the convergence conditions $D[\lambda_0^{max} - 4C\sin^2(\pi k/N)] < K$ hold, then all the decay terms in equations (16) and (17) will decrease to 0. We therefore lead the mean-squared values of $\|\eta\|^2 = \sum_{k=0}^{N-1} \|\eta_k\|^2$ to

$$\lg(\langle \|\eta\|^2 \rangle_t) = \lg\left(\left\langle \frac{1}{N} \sum_{k=0}^{N-1} \|\mathbf{DF}_a\|^2 \right\rangle_t\right) + 2\lg(\|\Delta\mathbf{a}\|) - 2\lg(K - \lambda_0^{max}) \tag{18}$$

and

$$\lg(\langle \|\eta\|^2 \rangle_t) \approx -\lg(K - \lambda_0^{max}) + \lg(\sigma^2) - \lg(2), \tag{19}$$

where $\langle \cdot \rangle_t$ denotes the average over time t . It is clear that chaotic synchronization will be influenced by noise, parameter mismatch, and the feedback weight K . Furthermore, $\langle \|\eta\|^2 \rangle_t$ increase with the increase of perturbation amplitudes, but decreases with the feedback weight K . It demonstrates that feedback can suppress the influences of noise and parameter mismatch. If K is significantly larger than λ_0^{max} , we can easily reduce equation (18) to $\|\eta\| \propto \|\Delta\mathbf{a}\|/K$. Obviously, compared with the relationship $\|\eta\| \propto \|\Delta\mathbf{a}\|$ of the Pecora–Carroll synchronization method [25], the feedback scheme shows a stronger robustness.

4. NUMERICAL CALCULATION OF COUPLED PARAMETRICALLY EXCITED PENDULUM ARRAYS

For the parametrically excited pendulum array, we have $\mathbf{u}_j = \{x_j, y_j\}^T$ and $\mathbf{F}(\mathbf{u}_j) = \{y_j - \beta y_j - [1 + p \cos(\omega t) \sin(x_j)]\}^T$. Here, x_j is the angular displacement, and y_j is the angular velocity. The system parameters can be written as $\mathbf{a} = \{\beta, p, \omega\}^T$. When $p = 2$, $\omega = 2$, $\beta = 0.1$, the single parametrically excited pendulum unit behaves as the tumbling chaos whose maximal Lyapunov exponent $\lambda_0^{max} \approx 0.34$ [26, 27]. The spatio-temporal

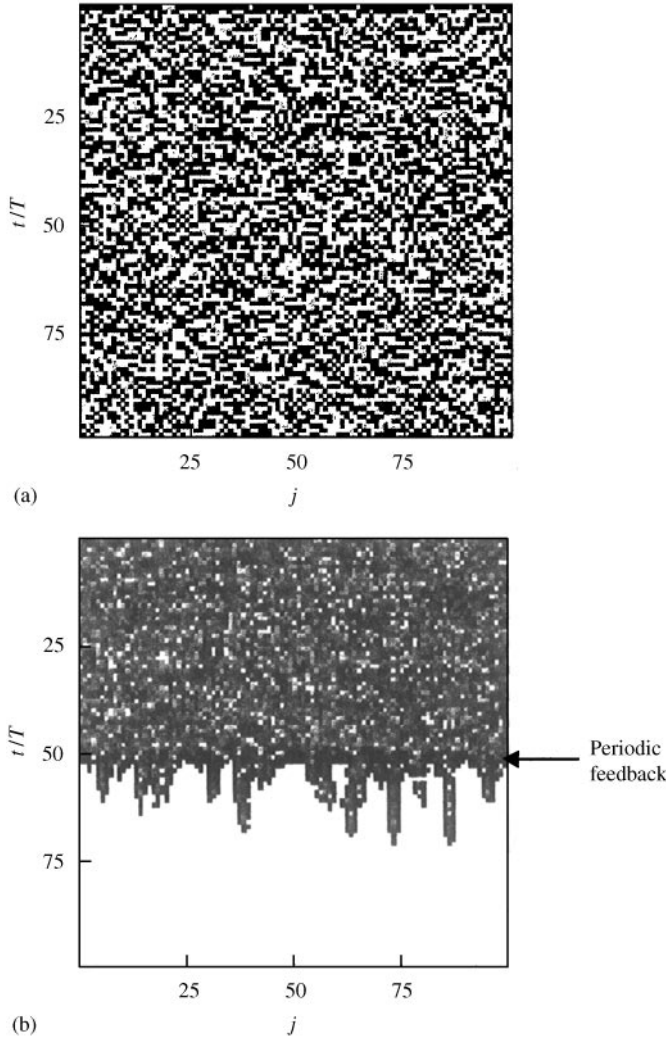


Figure 1. Spatio-temporal chaotic synchronization of the coupled parametrically excited pendulum arrays with periodic boundary condition by the periodic feedback method. (a) The spatio-temporal evolution x_j of the drive array with respect to the normalized time t/T and spatial co-ordinate j , where $C = 0.01$; (b) the difference $|x_j - \tilde{x}_j|$ of the drive and response arrays.

chaotic synchronization of the coupled parametrically excited pendulum arrays is illustrated in Figure 1. Figure 1(a) shows the evolution of the drive array where $C = 0.01$, and the gray-coded value of $x_j (j = 0, 1, \dots, 99)$ with respect to the normalized time t/T ($T = 2\pi/\omega$) and spatial co-ordinate j displays the space-time evolution. The drive array shows extreme irregularity in time and space. Imposing this spatio-temporal chaotic signal into the response array, we obtain the difference $|x_j - \tilde{x}_j| (j = 0, 1, \dots, 99)$ between the drive and response arrays (see Figure 1(b)). In our calculations, we take D as an integer number. To demonstrate how the periodic feedback method works, we do not activate the feedback between the two arrays at time $t = 0$ and allow the difference of state to be amplified (see the black and white regions). However, when $t > 50T$, feedback with $D = 10$ ($\tau_1 = 9T/200, \tau_2 = T/200$), $K = 10$ as activated. Two arrays will be synchronized well. The

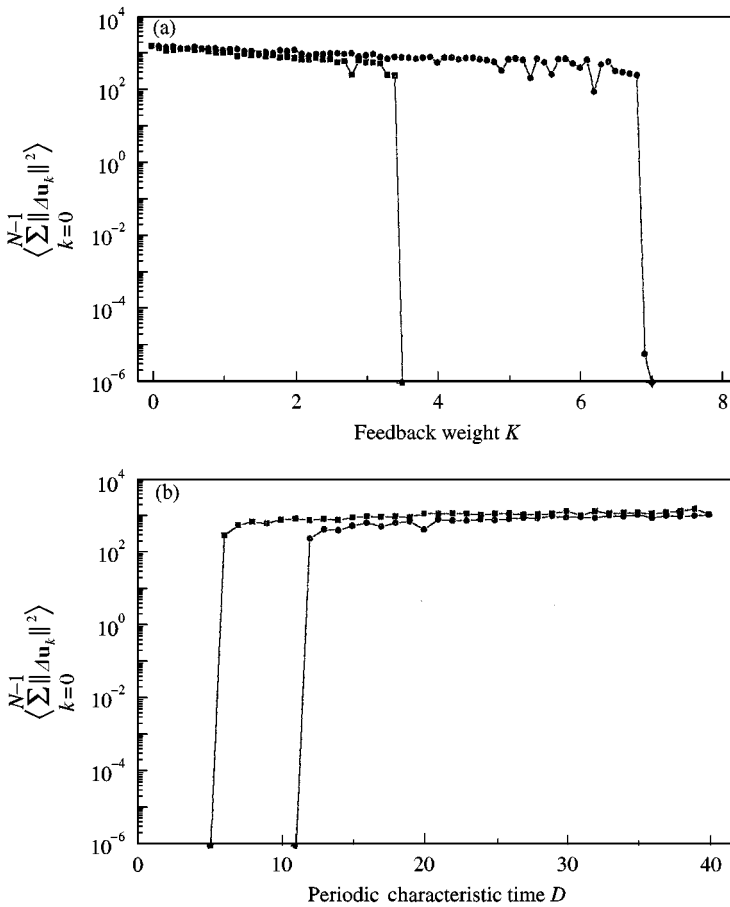


Figure 2. The dependence of the mean-squared value $\langle \sum_{k=0}^{N-1} \|\mathbf{u}_k - \tilde{\mathbf{u}}_k\|^2 \rangle$ on periodic characteristic time D and feedback weight K . (a) $\langle \sum_{k=0}^{N-1} \|\mathbf{u}_k - \tilde{\mathbf{u}}_k\|^2 \rangle \sim K$ where curves correspond to $D = 10, 20$, respectively (—■—, $D = 10$; —●—, $D = 20$); and (b) $\langle \sum_{k=0}^{N-1} \|\mathbf{u}_k - \tilde{\mathbf{u}}_k\|^2 \rangle \sim D$ where curves correspond to $K = 2, 4$ respectively, (—■—, $K = 2$; —●—, $K = 4$).

white region in Figure 1(b) indicates the synchronization of the two arrays. The critical values of the periodic characteristic time D_{max} and the feedback coupling parameter K_{min} can be obtained from the obvious jumps in the plots of the mean-squared value $\langle \sum_{k=0}^{N-1} \|\mathbf{u}_k - \tilde{\mathbf{u}}_k\|^2 \rangle$ versus D and K respectively. For example, in Figure 2(a), K_{min} associated with $D = 10, 20$ is 3.4 and 6.8 respectively. Figure 2(b) gives the critical value D_{max} associated with $K = 2, 4$ is 6 and 12 respectively. Compared with the results calculated by equation (14), it shows a good agreement between the numerical calculation and the theoretical prediction. When $K > K_{min}$ or $D < D_{max}$, the difference $\langle \sum_{k=0}^{N-1} \|\mathbf{u}_k - \tilde{\mathbf{u}}_k\|^2 \rangle$ decreases to zero so that synchronization is achieved.

In the practical application of synchronizing pendulums, the damping coefficient β , the exciting frequency parameter ω , and the exciting amplitude p are the main parameters that influence synchronization. Figure 3 shows the dependence of $\langle \sum_{k=0}^{N-1} \|\mathbf{u}_k - \tilde{\mathbf{u}}_k\|^2 \rangle$ on the feedback weight K of the parametrically excited pendulum arrays where we take 10% tolerance of the parameter difference. Figure 3(a)–(c) corresponds to parameter mismatch of $\Delta\omega = 0.2$, $\Delta p = 0.2$ and $\Delta\beta = 0.01$ where two curves are with respect to the periodic

characteristic times $D = 10, 20$ respectively. Figure 3(d) gives the relation between $\langle \sum_{k=0}^{N-1} \| \mathbf{u}_k - \hat{\mathbf{u}}_k \|^2 \rangle$ and the feedback weight K where the noise amplitude $\sigma = 0.1$.

Clearly, the numerical calculations as well as the theoretical analysis demonstrate that increasing K is very beneficial for suppressing the perturbations. The periodic feedback method is shown to have a strong robustness to noise and parameter mismatch in the realistic environment and is therefore recommended in a physical experiment.

The periodic synchronization scheme can also be generalized into synchronizing spatio-temporal chaotic arrays with other types of boundary condition. Considering the open boundary condition, we have the dynamics of coupled arrays.

Drive arrays

$$\begin{aligned}
 \dot{\mathbf{u}}_0 &= \mathbf{F}(\mathbf{u}_0, \mathbf{a}) + C\Gamma(\mathbf{u}_1 - \mathbf{u}_0), \\
 \dot{\mathbf{u}}_j &= \mathbf{F}(\mathbf{u}_j, \mathbf{a}) + C\Gamma(\mathbf{u}_{j+1} + \mathbf{u}_{j-1} - 2\mathbf{u}_j) \quad j = 1, 2, \dots, N - 2. \\
 \dot{\mathbf{u}}_{N-1} &= \mathbf{F}(\mathbf{u}_{N-1}, \mathbf{a}) + C\Gamma(\mathbf{u}_{N-2} - \mathbf{u}_{N-1}),
 \end{aligned}
 \tag{20}$$

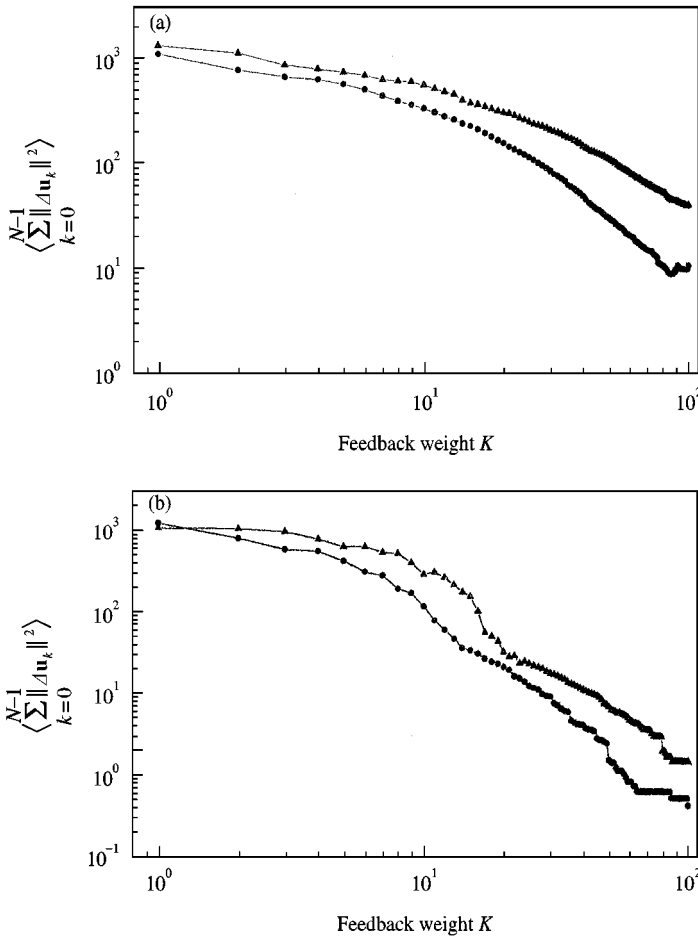


Figure 3. The influence of parameter mismatch and noise on chaotic synchronization where $D = 10$. (a)–(c) correspond to parameter mismatch $\Delta\omega = 0.2$, $\Delta p = 0.2$ and $\Delta\beta = 0.01$ respectively and (d) corresponds to noise with amplitude $\sigma = 0.1$ where the curves correspond to $D = 10, 20$ respectively. —●—, $D = 10$; —▲—, $D = 20$.

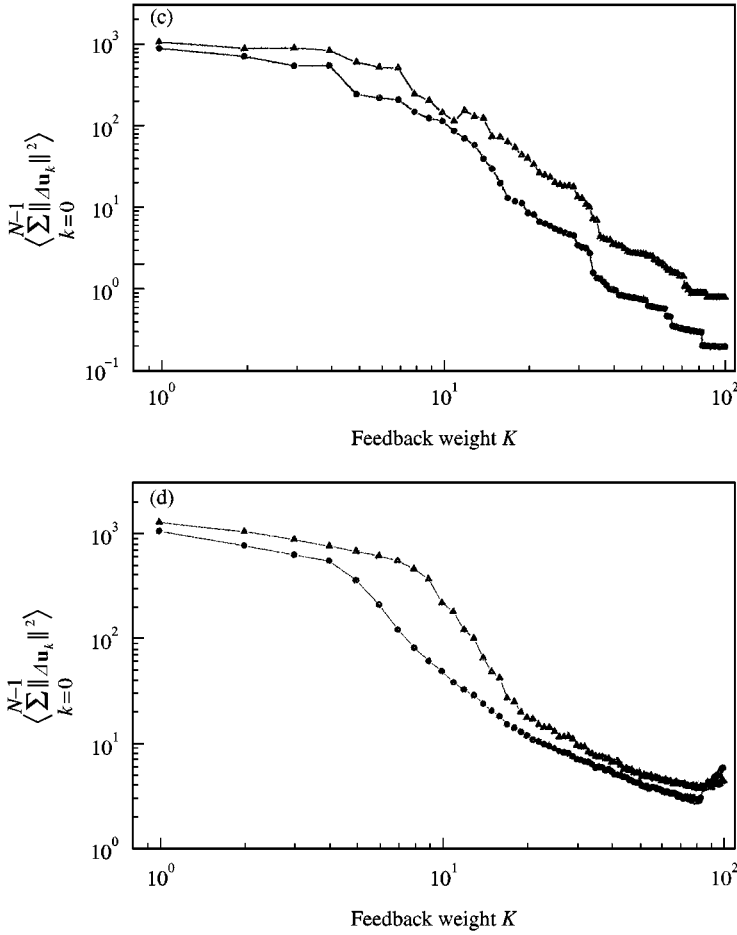


Figure 3. Continued.

Response array

$$\begin{aligned}
 \dot{\hat{\mathbf{u}}}_0 &= \mathbf{F}(\tilde{\mathbf{u}}_0, \tilde{\mathbf{a}}) + C\Gamma(\tilde{\mathbf{u}}_1 - \tilde{\mathbf{u}}_0) + K_f(t)\mathbf{I}(\mathbf{u}_0 - \tilde{\mathbf{u}}_0), \\
 \dot{\hat{\mathbf{u}}}_j &= \mathbf{F}(\tilde{\mathbf{u}}_j, \tilde{\mathbf{a}}) + C\Gamma(\tilde{\mathbf{u}}_{j+1} + \tilde{\mathbf{u}}_{j-1} - 2\tilde{\mathbf{u}}_j) + K_f(t)\mathbf{I}(\mathbf{u}_j - \tilde{\mathbf{u}}_j), \\
 \dot{\hat{\mathbf{u}}}_{N-1} &= \mathbf{F}(\tilde{\mathbf{u}}_{N-1}, \tilde{\mathbf{a}}) + C\Gamma(\tilde{\mathbf{u}}_{N-2} - \tilde{\mathbf{u}}_{N-1}) + K_f(t)\mathbf{I}(\mathbf{u}_{N-1} - \tilde{\mathbf{u}}_{N-1}),
 \end{aligned}
 \tag{21}$$

where we let $N = 120$,

$$\mathbf{I} = \Gamma = \begin{pmatrix} 0 & 0 \\ 0 & 1 \end{pmatrix}.$$

The spatio-temporal evolution of drive array and the synchronization of two arrays are given in Figure 4(a) and 4(b), respectively, where feedback weight $K = 10$ and periodic characteristic time $D = 2$. Figure 4(a) shows the irregular spatio-temporal characteristics of the drive array where the coupling constant $C = 0.01$, and the gray-coded value of x_j is with respect to time t and spatial coordinate j . The evolution of the difference $|x_j - \tilde{x}_j|$ is illustrated in Figure 4(b). Similarly, when $t < 50T$, we do not activate the feedback between the two array systems. So the difference of initial conditions will rapidly take effect (see the

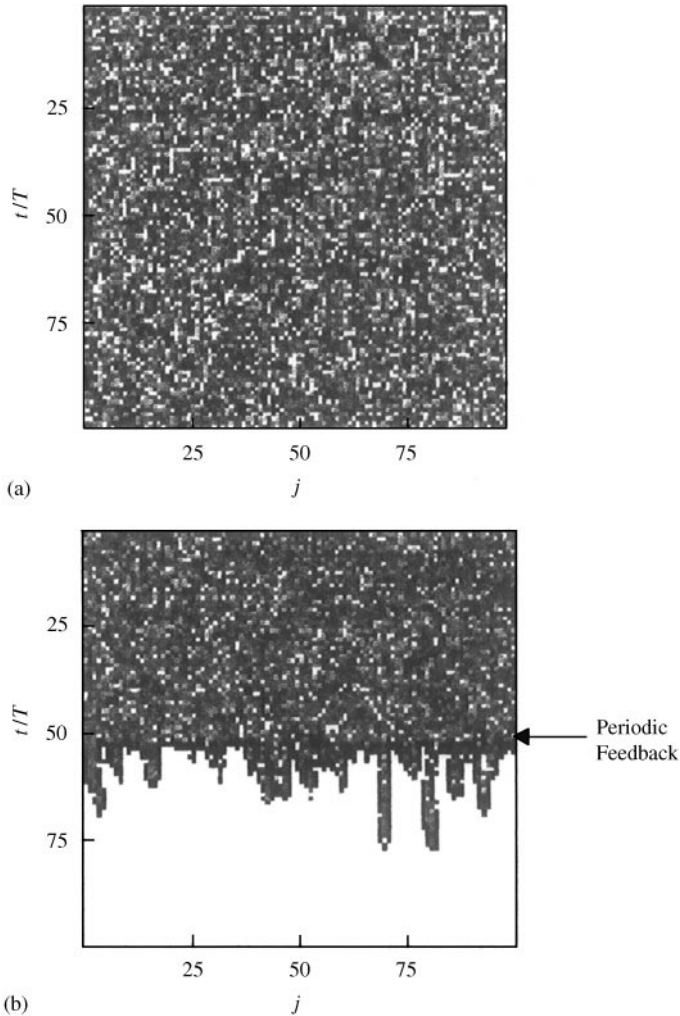


Figure 4. Spatio-temporal chaotic synchronization of the coupled parametrically excited pendulum arrays with open boundary condition by the periodic feedback method. (a) The spatio-temporal evolution x_j of the drive array with respect to the normalized time t/T and spatial co-ordinate j , where $C = 0.01$, and (b) the difference $|x_j - \tilde{x}_j|$ of the drive and response arrays.

black and white region in Figure 4(b)). The drive and response arrays behave independently as a kind of complex spatio-temporal pattern. After we switch on the feedback at $t > 50T$, spatio-temporal synchronization will be achieved. The white region in Figure 4(b) indicates that the differences between drive and response arrays will decrease to zero, then they are synchronous.

Finally, it should be noted that the present research dealing with spatio-temporal chaotic synchronization of parametrically excited pendulum arrays could also be applied to synchronize two single pendulum units. If we let the coupling constant $C = 0$, and the length of array $N = 1$, we can simplify the above results into synchronizing two chaotic pendulums. In reference [5], the periodic feedback method was applied to synchronize two parametrically excited pendulums numerically, whereas in this paper, chaotic synchronization by the periodic feedback method is given a more general description.

5. CONCLUSION

In this paper, we realize the spatio-temporal chaotic synchronization of parametrically excited pendulum arrays by the periodic feedback method. The synchronization condition was deduced in general coupled oscillator arrays. In order to make the synchronization method available in practical experiment, we investigated the influence of noise and parameter mismatch. We found that the periodic feedback method was robust in the presence of noise and parameter mismatch. The results provided potential applications of chaotic synchronization in practical environment. Finally, it should be mentioned that in our research, attention is focused on the global transverse stability of the synchronized state and synchronization is considered as the global behavior of chaotic systems. Therefore, the results are applicable for the general application of chaotic synchronization. Some recent researches demonstrate that high-quality synchronization should consider the local stability of the state if there exist locally unstable invariant sets in the synchronization manifold [28–30]. Otherwise, synchronization intervals will be interrupted by desynchronization events, which is called as attractor bubbling. This interesting phenomenon is also important and interesting for the high-quality synchronization of parametrically excited pendulums. Further research along this line is in the progress.

ACKNOWLEDGMENTS

The authors are very grateful to Prof. S. R. Bishop of University College London for his fruitful discussions.

REFERENCES

1. M. J. CLIFFORD and S. R. BISHOP 1994 *Journal of Sound and Vibration* **172**, 572–576. Approximating the escape zone for the parametrically excited pendulum.
2. R. W. LEVEN, B. POMPE, C. WILKE and B. P. KOCH 1985 *Physica D* **16**, 371–384. Experiments on periodic and chaotic motions of a parametrically forced pendulum.
3. S. R. BISHOP and M. J. CLIFFORD 1996 *Journal of Sound and Vibration* **189**, 142–147, Zones of chaotic behavior in the parametrically excited pendulum.
4. S. R. BISHOP, D. L. XU and M. J. CLIFFORD 1996 *Proceedings of the Royal Society of London A* **452**, 1789–1806. Flexible control of the parametrically excited pendulum.
5. Y. ZHANG, S. Q. HU and G. H. DU 1999 *Journal of Sound and Vibration* **223**, 247–254. Chaos synchronization of two parametrically excited pendulums.
6. H. G. WINFUL and L. RAHMAN 1990 *Physics Review Letters* **65**, 1575–1578. Synchronized chaos and spatiotemporal chaos in arrays of coupled lasers.
7. A. S. PIKOVSKY, M. G. ROSENBLUM and J. KURTHS 1996 *Europhysics Letters* **34**, 165–170. Synchronization in a population of globally coupled chaotic oscillators.
8. W. Z. CHEN 1994 *Physics Review B* **49**, 15 063–15 066. Experimental observation of solutions in 1D nonlinear lattice.
9. Y. C. LAI and C. GREBOGI 1994 *Physics Review E* **50**, 1894–1899. Synchronization of spatiotemporal chaotic systems by feedback control.
10. L. M. PECORA and T. L. CARROLL 1990 *Physics Review Letters* **64**, 821–823. Synchronization in chaotic system.
11. K. PYRAGAS 1993 *Physics Letters A* **181**, 203–210. Predictable chaos in slightly perturbed unpredictable chaotic systems.
12. K. M. CUOMO and A. V. OPPENHEIM 1993 *Physics Review Letters* **71**, 65–68. Circuit implementation of synchronized chaos with applications to communications.
13. L. KOCAREV and U. PARLITZ 1995 *Physics Review Letters* **74**, 5028–5031. General approach for chaotic synchronization with application to communication.

14. T. YANG, W. W. CHAI and L. O. CHUA 1997 *IEEE Transactions on Circuits* **44**, 469–472. Cryptography based on chaotic systems.
15. Y. ZHANG, J. M. YU and G. H. DU 1998 *Chinese Science Bulletin* **43**, 1519–1523. Secure communication by small time continuous feedback.
16. M. DAI, Y. ZHANG, Y. M. HUA, W. S. NI and G. H. DU 1998 *Electronic Letters* **34**, 951–953. Implementation of secure digital communication by hyperchaotic synchronization.
17. Y. ZHANG, M. DAI, Y. M. HUA, W. S. NI and G. H. DU 1998 *Physics Review E* **58**, 3022–3027. Digital communicated by active–passive-decomposition synchronization in hyperchaotic systems.
18. Y. ZHANG, M. DAI, Y. M. HUA and G. H. DU 1999 *Electronics Letters* **35**, 2087–2089. Hyperchaotic synchronisation scheme for digital speech communication.
19. L. KOCAREV and U. PARLITZ 1996 *Physics Review Letters* **77**, 2206–2209. Synchronizing spatiotemporal chaos in coupled nonlinear oscillators.
20. J. F. HEAGY, L. M. PECORA and T. L. CARROLL 1995 *Physics Review Letters* **74**, 4185–4188. Short wavelength bifurcations and size instabilities in coupled oscillator systems.
21. J. F. HEAGY, T. L. CARROLL and L. M. PECORA 1994 *Physics Review E* **50**, 1874–1885. Synchronous chaos in coupled oscillator systems.
22. J. Z. YANG, G. HU and J. H. XIAO 1998 *Physics Review Letters* **80**, 496–499. Chaos synchronization in coupled chaotic oscillators with multiple positive Lyapunov exponents.
23. M. N. LORANZO, I. P. MARINO, V. P. MUNUZURI, M. A. MATIAS and V. P. VILLAR 1996 *Physics Review E* **54**, 3094–3099. Synchronization waves in arrays of driven chaotic systems.
24. H. G. SCHUSTER, S. MARTIN and W. MARTINSEN 1986 *Physics Review A* **33**, 3547–3549. New method for determining the largest Liapunov exponent of simple nonlinear systems.
25. L. M. PECORA and T. L. CARROLL 1991 *Physics Review A* **44**, 2374–2383. Driving systems with chaotic signals.
26. R. V. DOOREN 1997 *Journal of Sound and Vibration* **200**, 105–109, Comments on “Zones of chaotic behavior in the parametrically excited pendulum”.
27. S. R. BISHOP and M. J. CLIFFORD 1997 *Journal of Sound and Vibration* **200**, 109–110. Author’s reply.
28. D. J. GAUTHIER and J. C. BIENFANG 1996 *Physics Review Letters* **79**, 1751–1754. Intermittent loss of synchronization in coupled chaotic oscillators: Toward a new criterion for high-quality synchronization.
29. N. F. RULKOV and M. M. SUSHCHIK 1997 *International Journal of Bifurcation and Chaos* **7**, 625–643. Robustness of synchronized chaotic oscillations.
30. L. M. PECORA and T. L. CARROLL 1999 *International Journal of Bifurcation and Chaos* **9**, 2315–2320. Mast stability functions for synchronized coupled systems.